

# Nitroanilines as Quenchers of Pyrene Fluorescence

Carlos E. Agudelo-Morales,<sup>[a]</sup> Oscar F. Silva,<sup>[a]</sup> Raquel E. Galian,<sup>\*[a, b]</sup> and Julia Pérez-Prieto<sup>\*[a]</sup>

The quenching of pyrene and 1-methylpyrene fluorescence by nitroanilines (NAs), such as 2-, 3-, and 4-nitroaniline (2-NA, 3-NA, and 4-NA, respectively), 4-methyl-3-nitroaniline (4-M-3-NA), 2-methyl-4-nitroaniline (2-M-4-NA), and 4-methyl-3,5-dinitroaniline (4-M-3,5-DNA), are studied in toluene and 1,4-dioxane. Steady-state fluorescence data show the higher efficiency of the 4-NAs as quenchers and fit with a sphere-of-action model. This suggests a 4-NA tendency of being in close proximity to the fluorophore, which could be connected with their high polarity/hyperpolarizability. In addition, emission and excitation spectra evidence the formation of emissive pyrene–NA ground-state complexes in the case of the 4-NAs and, in a minor degree, in the 2-NA. Moreover, time-resolved fluores-

cence experiments show that increasing amounts of NA decrease the pyrene fluorescence lifetime to a degree that depends on the NA nature and is larger in the less viscous solvent (toluene). Although the NA absorption and the pyrene (Py) emission overlap, we found no evidence of dipole–dipole energy transfer from the pyrene singlet excited state (<sup>1</sup>Py) to the NAs; this could be due to the low NA concentration used in these experiments. Transient absorption spectra show that the formation of the pyrene triplet excited state (<sup>3</sup>Py) is barely affected by the presence of the NAs in spite of their efficiency in <sup>1</sup>Py quenching, suggesting the involvement of <sup>1</sup>Py–NA exciplexes which—after intersystem crossing—decay efficiently into <sup>3</sup>Py.

## 1. Introduction

Nitroanilines (NAs) are intermediates in the synthesis of dyes, pesticides, and pharmaceuticals, and they are reduction products of aromatic explosives. They have been used as fluorescence quenchers of organic chromophores (pyrochlorophyll, benzo[k]fluoranthene, anthracene), biomacromolecules (bovine serum albumin), as well as nanomaterials (cobalt 8-hydroxyquinoline complex-based nanosheets).<sup>[1–4]</sup> In fact, some of these fluorescent systems have been used as isomeric aromatic amine probes.<sup>[5,6]</sup> In addition, the capacity of NAs as quenchers has been applied to the direct characterisation of micellar properties of surfactants containing a fluorophore.<sup>[7]</sup>

Nitroanilines are highly polar molecules belonging to a type of substituted aromatic molecules with a donor–aromatic–acceptor structure. The ground-state dipole moment ( $\mu$ ) of 2-nitroaniline (2-NA), 3-nitroaniline (3-NA), and 4-nitroaniline (4-NA) is about 4.7, 5.7, and 7.2 D, respectively,<sup>[8,9]</sup> in dioxane (see Table S1 of the Supporting Information). The lowest-energy absorption band of 3-NA, 2-NA, and 4-NA is located at quite dissimilar wavelengths ( $\lambda_{\text{max}}$  at 348, 377, and 322 nm, respectively) and exhibits a considerably different molar absorption coefficient (values of 2200, 4800, and 12600  $\text{m}^{-1} \text{cm}^{-1}$ , respectively, in methylcyclohexane).<sup>[10]</sup> It has been suggested that the quenching of the fluorescence of aromatic compounds by NAs can have a static or dynamic nature and can occur via electron or energy transfer. Moreover, the involvement of transient fluorophore–NA complexes (exciplexes), which decay by electron transfer, intersystem crossing, or internal conversion, has been postulated. On many occasions, the behaviour of isomeric NAs, such as 2-, 3-, and 4-NA, as quenchers has been compared with that of aromatic nitrated explosives which act as electron acceptors, though the relative quenching efficiency of the isomeric NAs did not correlate well with their relative redox po-

tential, which decreases in the order 3-NA > 2-NA > 4-NA, Table S1 of the Supporting Information.<sup>[11]</sup>

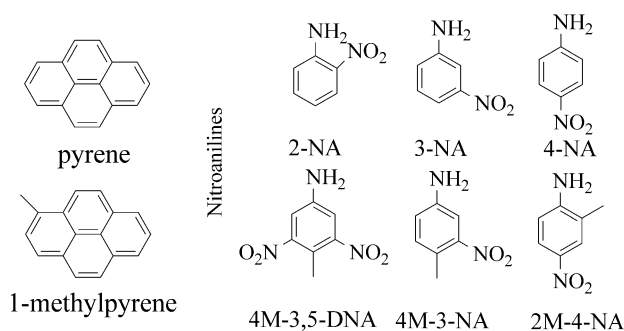
Therefore, a systematic study on the interaction between a well-known and extensively used fluorophore, such as pyrene, and NAs would be of interest to gain insight into their role as quenchers. Pyrene has been widely used as a probe due to 1) its absorption (strength) features, 2) its long singlet lifetime (> 100 ns,<sup>[12,13]</sup> and the information that can be obtained from its fluorescence emission ( $I_3/I_1$  ratio),<sup>[14,15]</sup> and 3) its long-lived triplet excited state (microsecond scale). This chromophore has been used in fluorescent chemosensors that can recognize selectively chemical species in potential analytical applications.<sup>[16,17,18]</sup> In fact, nitrated explosives have been detected by fluorescence quenching of pyrene and related compounds.<sup>[19,20]</sup>

We report herein on the quenching of pyrene and 1-methylpyrene fluorescence by unsubstituted NAs (2-, 3-, and 4-NA), methylnitroanilines (4-methyl-3-nitroaniline, 4-M-3-NA, and 2-methyl-4-nitroaniline, 2-M-4-NA), and a dinitroaniline (4-methyl-3,5-dinitroaniline, 4-M-3,5-DNA) in toluene and 1,4-dioxane

[a] C. E. Agudelo-Morales, Dr. O. F. Silva, Dr. R. E. Galian, Prof. J. Pérez-Prieto  
Molecular Science Institute (ICMol)  
University of Valencia, C/Catedrático José Beltrán 2  
46980 Paterna, Valencia (Spain)  
Fax: (+34) 963543274  
E-mail: Julia.perez@uv.es

[b] Dr. R. E. Galian  
Department of Analytical Chemistry  
University of Valencia, C/Dr. Moliner 50  
46100 Burjassot, Valencia (Spain)  
E-mail: Raquel.galian@uv.es

Supporting information for this article is available on the WWW under <http://dx.doi.org/10.1002/cphc.201200637>.



**Scheme 1.** Structure of the pyrenes and nitroanilines studied herein.

(Scheme 1). Steady-state fluorescence data revealed positive deviation from linearity in the Stern–Volmer (SV) plots for some NAs. Time-resolved absorption and fluorescence studies were used to gain insight into the quenching mechanism and the species involved in this process. These studies show the tendency of NAs to establish specific interactions with the pyrene singlet excited state and, depending on their structure, to be adjacent to the fluorophore at the ground state, some forming a ground state complex.

## 2. Results and Discussion

### 2.1. Steady-State Absorption and Fluorescence Studies

Comparison of the pyrene and methylpyrene (31 and 37  $\mu\text{M}$ , respectively) absorption spectra with those of each of the unsubstituted NAs (40  $\mu\text{M}$ ) and the corresponding pyrene/NA mixture was registered in both toluene (see Figure 1) and dioxanes (Figure not shown). The absorption spectrum of each mixture was a simple addition of the spectra of the components, that is, the NAs and the pyrenes. The overlap between the pyrene absorption and that of the NA was considerable in the case of the 4-NAs.

Steady-state fluorescence studies showed that the NAs are strong quenchers of the pyrene fluorescence emission. Figure 2 shows the emission spectra of deaerated toluene solutions of pyrene and 1-methylpyrene (pyrene: 31  $\mu\text{M}$ ,  $\lambda_{\text{exc}} = 337 \text{ nm}$ ; 1-methylpyrene: 37  $\mu\text{M}$ ,  $\lambda_{\text{exc}} = 345 \text{ nm}$ ) in the presence

of increasing amounts, up to 40  $\mu\text{M}$ , of 2-, 3-, and 4-NA, corrected by the quencher absorbance at the excitation wavelength (for details of the inner filtering corrections see the Supporting Information). With regards to the substituted NAs, their absorption and emission spectra in toluene are shown in Figures S1 and S2 of the Supporting Information.

The area under the pyrene emission curve was registered in the presence and in the absence of increasing amounts of NA ( $I_0$  and  $I$ , respectively), and the  $I_0/I$  ratios were plotted versus the NA concentration [NA]. The  $I_0/I$  ratio showed a linear dependence on [3-NA] and an upward dependence on [2-NA] and [4-NA] (Figure 3A, Figure 3C). The behaviour of 2-M-4-NA was similar to that of 4-NA, while that of 4-M-3-NA and 4-M-

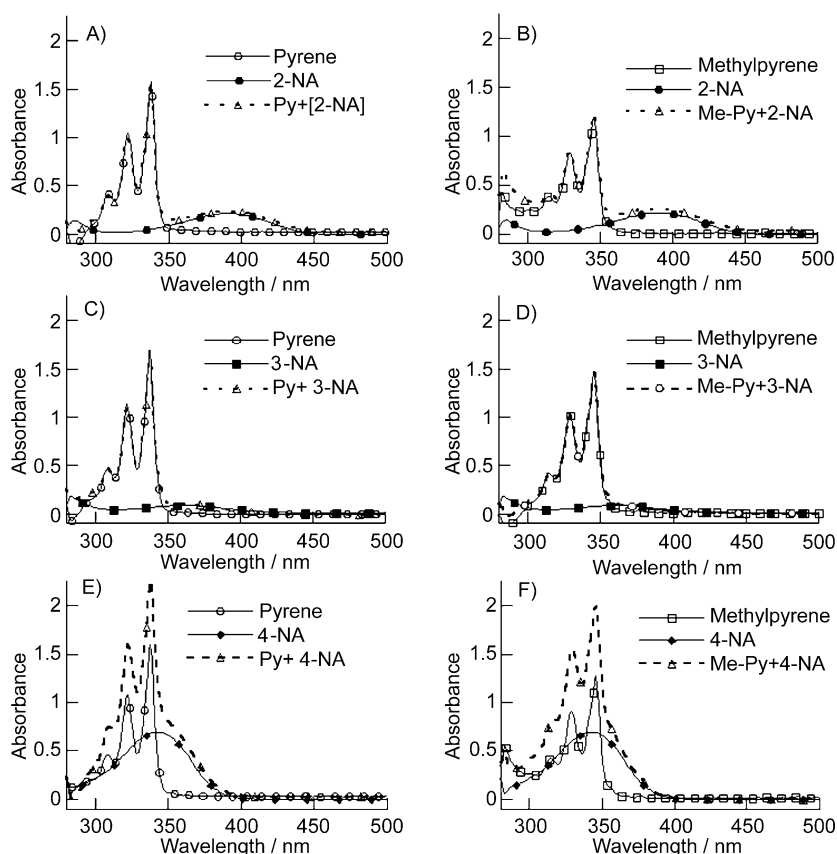


**Figure 1.** A–C) Absorption spectra of toluene solutions of pyrene (31  $\mu\text{M}$ ), NA (40  $\mu\text{M}$ ), and a pyrene/NA mixture (31  $\mu\text{M}$ /40  $\mu\text{M}$ ), and spectrum obtained by addition of the NA and pyrene spectra. B–F) Absorption spectra of toluene solutions of 1-methylpyrene (37  $\mu\text{M}$ ), NA (40  $\mu\text{M}$ ), and a methylpyrene/NA mixture (37  $\mu\text{M}$ /40  $\mu\text{M}$ ), and spectrum obtained by addition of the NA and methylpyrene spectra. The names of the NA isomer and the pyrene derivative are depicted on each graph.

3,5-DNA was analogous to that of 3-NA (Figures 3A and 3C show the SV plots for pyrene and 1-methylpyrene in toluene; for results in dioxane see Figures S3A and S3C of the Supporting Information).

Since 2-NA and 4-NAs have considerable absorption in the emission spectral region, the pyrene emission was also registered at a fixed wavelength (pyrene:  $\lambda_{\text{em}} = 364 \text{ nm}$ ; 1-methylpyrene:  $\lambda_{\text{em}} = 368 \text{ nm}$ ) in the presence and in the absence of increasing amounts of the NA. Then, the emission intensities

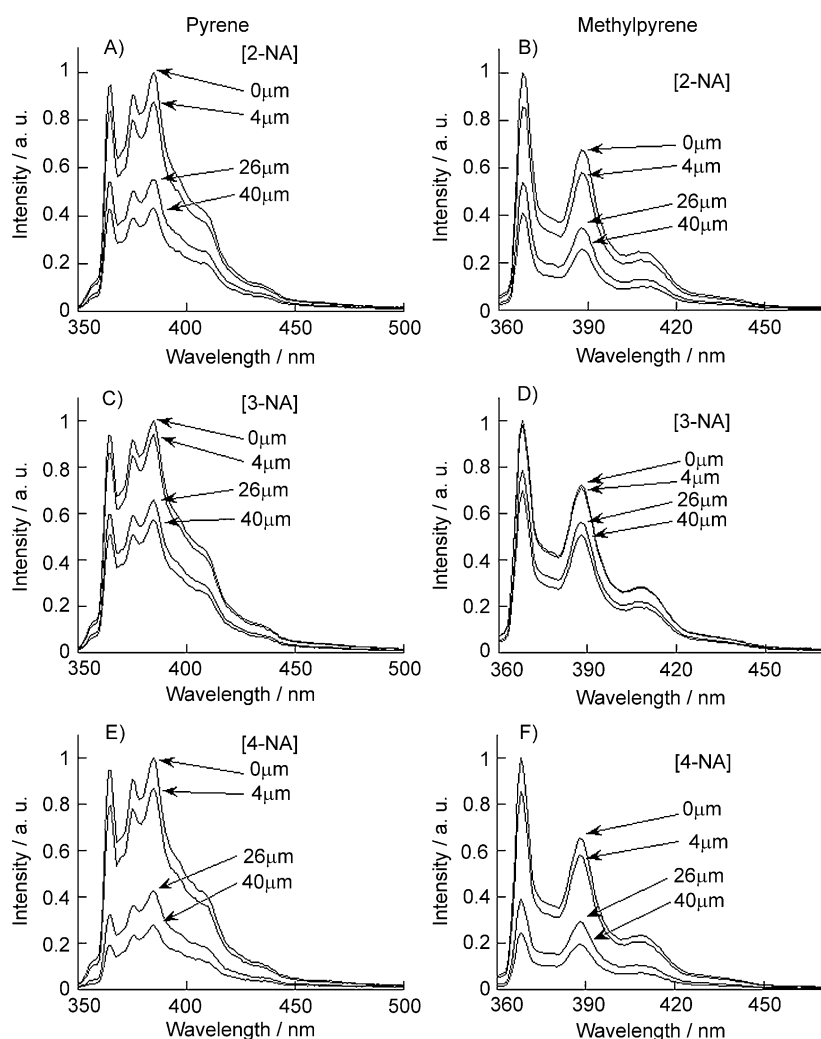


**Figure 2.** A–E) Emission spectra ( $\lambda_{\text{exc}} = 337$  nm) of deaerated toluene solutions of pyrene ( $31 \mu\text{M}$ ) in the presence of increasing amounts of NA (up to  $40 \mu\text{M}$ ). B–F) Emission spectra ( $\lambda_{\text{exc}} = 345$  nm) of deaerated toluene solutions of methylpyrene ( $37 \mu\text{M}$ ) in the presence of increasing amounts of NA (up to  $40 \mu\text{M}$ ). The structure of the NA isomer is depicted on each graph. The emission spectra were corrected by the quencher absorbance at the excitation wavelength.

were corrected by the quencher absorbance at both the excitation and the emission wavelength. Again, the plots of  $I_0/I$  ratios versus [NA] showed an upward dependence of the fluorophore emission on the NA concentration (see Figure S4, Supporting Information).

A linear SV relationship can be observed if either static or dynamic quenching occurs, in which case SV Equation (1) can be used to quantify the analyte quenching efficiency:

$$I_0/I = 1 + K[Q] \quad (1)$$

In this equation,  $I_0$  and  $I$  are the emission intensities in the absence and presence of the quencher (Q), respectively; [Q] is the molar concentration of Q; and  $K$  is the SV constant which, in the case of static quenching, is the association constant ( $K_a$ ) between the fluorophore (F) and Q.

If the quenching is dynamic,  $K$  is the dynamic quenching constant ( $K_d$ ). Data of  $I_0/I$  versus [3-NA] fitted well to Equa-

tion (1), as it did in the other 3-NAs (Figures 3A and 3C in toluene and figures S3A and S3C, Supporting Information, in dioxane), suggesting a predominant static or dynamic quenching.

Equation (1) applies for a limited range of small and moderate  $K_a$  values, except for a very high [Q] where  $[Q] \gg [F]$ . This equation for static quenching is a simplification of the general Equation (2) for pure static quenching:

$$I_0/(I_0 - I) = 1/K_a[Q] + 1/f_f \quad (2)$$

where  $(I_0 - I)$  refers to the change in fluorescence intensity on the addition of a Q,  $f_f$  refers to the fraction of F fluorescence quenched by Q, and  $K_a$  is the binding constant in the F–Q complex. Therefore, it should be taken into account that pure static quenching by complexation could lead to upward curvatures in the SV plots. Therefore, the data of pyrene fluorescence quenching by 2-, and 4-NAs were analysed using Equation (2), but they did not fit well to pure static quenching. So, the SV plots for these quenchers were subsequently analysed in terms of combined dynamic and static quenching [Eq. (3)], but neither did the data fit well to this model:

$$I_0/I = (1 + K_d[Q])(1 + K_a[Q]) \quad (3)$$

Remarkably, the up-curving plots for 2-, and 4-NAs fitted well to the Perrin static quenching model [Eq. (4)]:

$$\ln(I_0/I) = K_{\text{ap}}[Q] \quad (4)$$

where  $K_{\text{ap}}$  is the apparent static quenching constant (see Figures 3B and 3D in toluene and Figures S3B and S3D, Supporting Information, in dioxane). In this model, static quenching occurs between randomly distributed fluorophores and quenchers that are located in the proximity (action volume). Fluorophore molecules in contact with Q at the instant of excitation will not fluoresce. At best, they have a non-unit probability of fluorescing if the quenching reaction is not totally efficient. Some

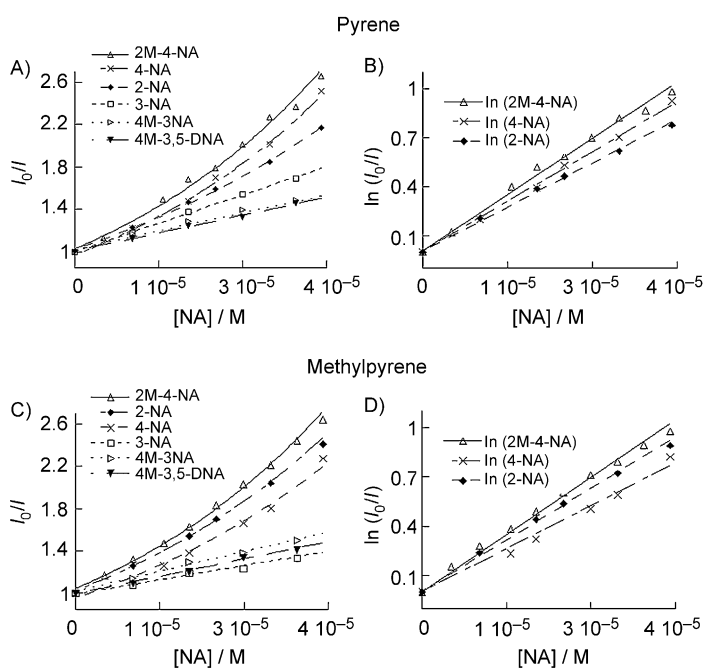


**Figure 3.** Stern–Volmer graphs of the fluorescence quenching of pyrene (A,  $\lambda_{\text{exc}}=337$  nm) and methylpyrene (C,  $\lambda_{\text{exc}}=345$  nm) in deoxygenated toluene solutions at room temperature upon addition of increasing quantities of the nitroaniline. Fitting of the data of 2-, and 4-NAs to the Perrin static model (B: pyrene; D: methylpyrene). The emission intensities were corrected by the quencher absorbance at the excitation wavelength.

of the fluorophore molecules will be quenched in a diffusion-dependent manner.

Close observation of the shape of the pyrene emission spectrum under increasing amounts of the NAs (up to ca. 40  $\mu\text{M}$ ) revealed changes in the  $I_3/I_1$  ratio ( $I_1$  at 364 nm and  $I_3$  at 384 nm) of the pyrene emission bands in some cases (see Figure 4 and Figure S5, Supporting Information, for pyrene re-

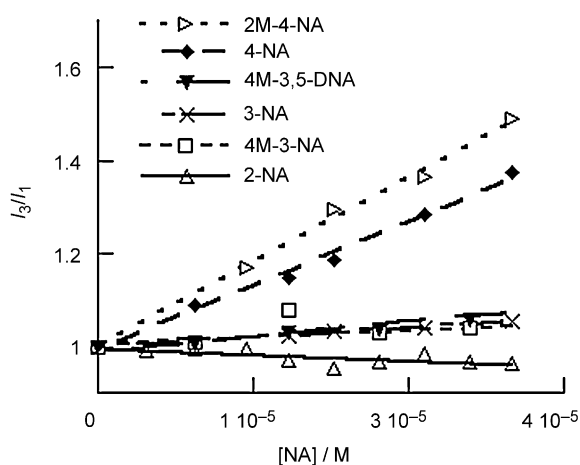


**Figure 4.** Change in the  $I_3/I_1$  ratio of the pyrene emission bands in deaerated toluene solutions in the presence of increasing amounts of the indicated nitroanilines ( $\lambda_{\text{exc}}=337$  nm). The emission intensities were corrected by the quencher absorbance at the excitation wavelength.

sults in toluene and dioxane, respectively). This ratio did not change in the presence of increasing amounts of 3-NA, 4-M-3-NA, and 4-M-3,5-DNA, although it decreased slightly in the case of 2-NA but increased significantly in the 4-NAs (4-NA and 2-M-4-NA).

Subsequently, the emission spectra of methylpyrene/4-NA mixtures at  $\lambda_{\text{ex}}=345$  nm were normalised at 364 nm, where the least amount of emission interference occurred. The differential emission spectrum obtained by subtracting the fluorescence spectrum of methylpyrene from that of a methylpyrene/4-NA (37  $\mu\text{M}/40$   $\mu\text{M}$ ) mixture showed the features of the new emission extending from 375 to 450 nm and a  $\lambda_{\text{max}}$  of about 380 nm, that is, red-shifted compared with that of methylpyrene (see Figure 5 in dioxane). Similar observations were found in the case of pyrene (Figure not shown).

Changes in the  $I_3/I_1$  ratio of the pyrene emission bands could be due to the formation of emissive  $^1\text{Py-NA}$  exciplexes ( $^1\text{Py-NA}$ ), arising from the interaction of the pyrene singlet excited state with the NA ground state<sup>[21–24]</sup> (Scheme 2). Alternatively, the species responsible for such changes could be  $^1(\text{Py-NA})$  complexes obtained after excitation of  $\text{Py-NA}$  ground-state complexes (Scheme 2). Addi-

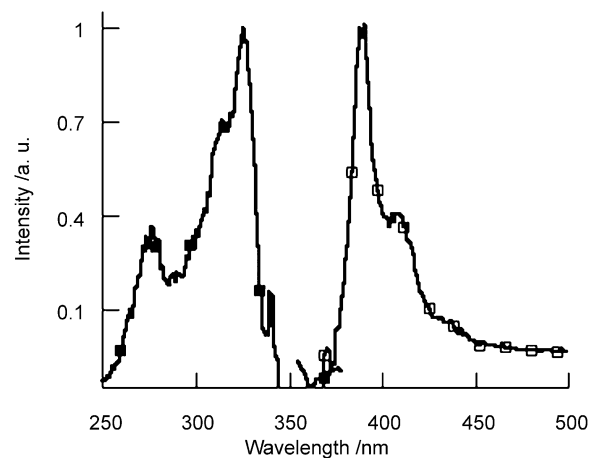
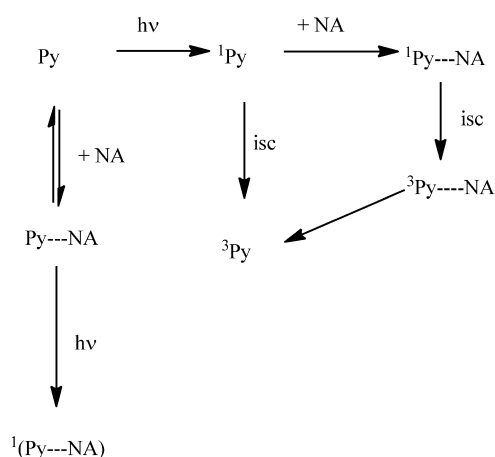


**Figure 5.** Left: Differential excitation spectra ( $\lambda_{\text{em}}=364$  nm) of a mixture of methylpyrene/4-NA (37  $\mu\text{M}/40$   $\mu\text{M}$ ) in deaerated dioxane. Right: Differential emission spectra ( $\lambda_{\text{exc}}=345$  nm) of a mixture of methylpyrene/4-NA (37  $\mu\text{M}/40$   $\mu\text{M}$ ) in deaerated dioxane.

tionally, the NA capacity to affect the local environment of pyrene could be the sole factor that determines the change in the  $I_3/I_1$  ratio of the pyrene emission bands. Excitation spectra were used to elucidate the nature of the emissive species: the  $^1(\text{Py-NA})$  complex would lead to the spectrum of the  $\text{Py-NA}$  ground-state complex; the  $^1\text{Py-NA}$  exciplex would lead to the pyrene spectrum; and similar results would be found if the NAs affect the local environment of pyrene and are responsible for the  $I_3/I_1$  ratio change.



**Scheme 2.** Relevant processes in the quenching of pyrene by nitroanilines.

The excitation spectra ( $\lambda_{em}=364$  nm) of methylpyrene/4-NA mixtures in dioxane were normalised at 343 nm. The differential excitation spectrum obtained by subtracting the excitation spectrum of methylpyrene from that of a methylpyrene/4-NA ( $37 \mu\text{M}/40 \mu\text{M}$ ) mixture showed the features of a new species, whose longest wavelength absorption band was between 250 and 340 nm with a  $\lambda_{max}$  at about 320 nm (Figure 5). This finding rules out that the new emission arises from an emissive  $^1\text{Py}-4\text{-NA}$  exciplex and suggests the formation of a  $\text{Py}-4\text{-NA}$  ground-state complex. Similar analyses were performed to obtain the absorption and emission features of the  $\text{Py}-2\text{-NA}$  ground-state complex (not shown).

Though the excitation spectra evidenced the formation of  $\text{Py}-\text{NA}$  ground-state complexes, mainly in the case 4-NA, these

species were not detected by absorption spectroscopy. This suggests that these species were generated in a very low concentration and/or had a low molar absorption coefficient.

The quenching efficiency by the NAs was slightly influenced by the solvent nature (toluene vs. 1,4-dioxane) and the pyrene substitution (pyrene vs. 1-methylpyrene), but it was greater for the 4-NAs than for the others (see Figure 6, top, and Figure S6 and Table S2 of the Supporting Information).

## 2.2. Time-Resolved Fluorescence Studies

Time-resolved fluorescence measurements were determined to gain insight into the static and/or dynamic nature of pyrene fluorescence quenching by NAs. The data were analysed using Equation (5):

$$\tau_0/\tau = 1 + K_d[\text{Q}] = 1 + k_q\tau_0[\text{Q}] \quad (5)$$

where  $k_q$  is the quenching rate constant, and  $\tau$  and  $\tau_0$  are the lifetimes of the excited species in the absence and presence of Q. These studies confirmed that quenching of pyrene fluorescence by 3-NA and 4-M-3-NA was predominantly dynamic (Figure 7B in toluene). The quenching of the pyrene emission by 2-NA also exhibited a considerably dynamic contribution (Figure 7A). By contrast, it had a considerably static contribution for 4-M-3,5-DNA (Figure 7C). Finally, the high contribution of apparent static quenching was confirmed for the 4-NAs, that is, 2-M-4-NA and 4-NA (Figure 7D).

The quenching rate constants showed a drastic dependence on the solvent nature (Figure 6, bottom, and Table S2 of the Supporting Information). Toluene and 1,4-dioxane have similar dipole moments (0.31 and 0.45 Debye, respectively) but differ

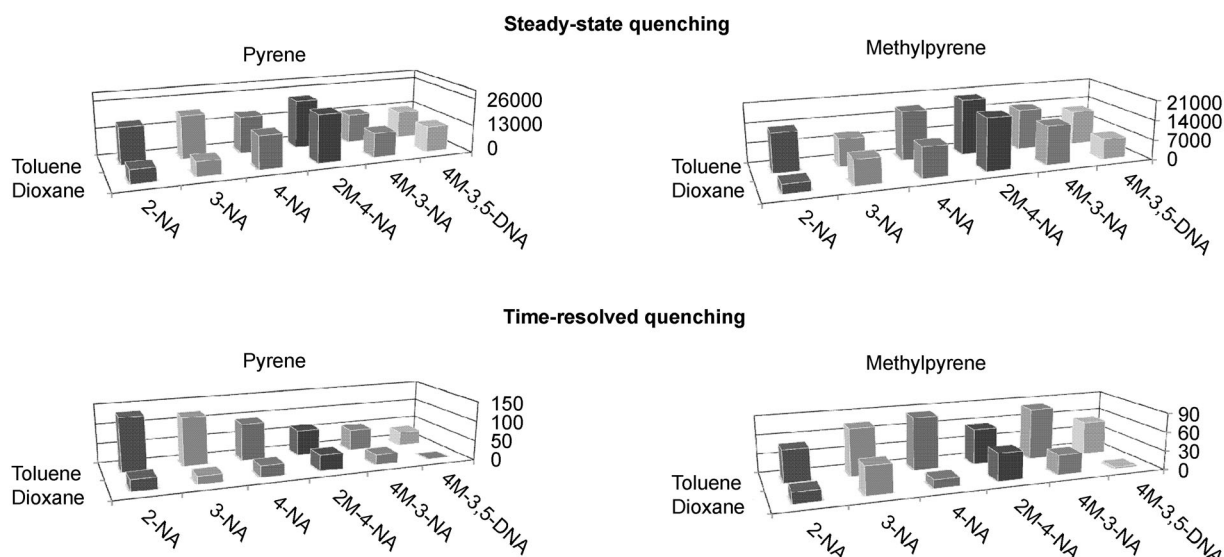


**Figure 6.** Top: Comparison of the quenching constants of pyrene (left) and 1-methylpyrene (right) emission in toluene and dioxane by NAs; the constants were obtained from the steady-state studies. The emission intensities were corrected by the quencher absorbance at the excitation wavelength. Bottom: Comparison of the quenching rate constants of pyrene (left) and 1-methylpyrene (right) emission by NAs in toluene and dioxane; the rate constants were obtained from the time-resolved studies.

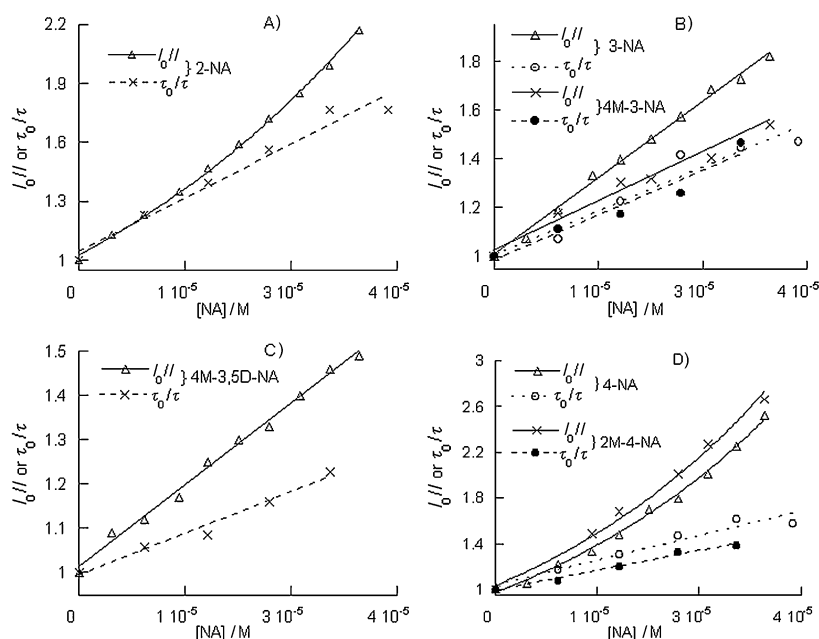


**Figure 7.** Stern–Volmer plots showing a comparison between the intensity (—) and the lifetime (---,  $\lambda_{em}$  at 364 nm) dependence of pyrene emission in toluene on the NA concentration.

significantly in their viscosity (ca. 0.5 and 1.1 cP, respectively).<sup>[25]</sup> The remarkable decrease in the rate constants in the more viscous dioxane was consistent with the diffusion-dependent nature of such quenching. In addition, the rate constants also showed a considerable dependence on the pyrene substitution. This indicated the occurrence of specific interactions between the fluorophore singlet excited state and the NA.

### 2.3. Control Studies

The 3-NA could be an acceptor of pyrene singlet energy, since there was a large spectral overlap between its absorption spectrum and that of the pyrene emission (Figure S7, Supporting Information). This NA exhibited fluorescence in dioxane and toluene at room temperature; thus, its emission spectrum presented a broad band between 450 and 626 nm with  $\lambda_{max}$  at 480 nm (Figure S8, Supporting Information). This spectrum was similar to that reported for 3-NA at low temperatures.<sup>[26,27]</sup> Control studies showed that the emission of 3-NA did not increase in the presence of pyrene (Figure not shown), which indicated that a dipole–dipole singlet–singlet energy-transfer mechanism did not contribute significantly to the pyrene fluorescence quenching. It should be taken into account that for unlinked donor/acceptor pairs, the acceptor concentration must be quite high for the occurrence of significant energy transfer by such mechanism and both the potential energy acceptor [NA] and the donor concentrations were kept below 40  $\mu\text{M}$  in our experiments. Transient absorption spectroscopy could be used to gain information about the consequences of the pyrene fluorescence quenching by NAs on the pyrene triplet ( $^3\text{Py}$ ) yield. Remarkably, laser flash photolysis (Nd:YAG, 355 nm, 10 ns pulse) of the pyrenes showed that the  $^3\text{Py}$  absorbance was little affected by the presence of 3-NA, in spite of efficient

quenching of  $^1\text{Py}$  by this NA (Figure S9, Supporting Information).

This finding suggests an enhanced intersystem crossing to the  $^3\text{Py}$  via  $^1\text{Py}$ –3-NA exciplexes or triplet–triplet energy transfer from the 3-NA triplet excited state ( $^3\text{3-NA}$ ) to Py (Scheme 2). Laser flash photolysis of 3-NA gave rise to a transient with an absorption band between 360 and 540 nm ( $\lambda_{max}$  ca. 460 nm) and a lifetime of 1.6  $\mu\text{s}$  in toluene (Figure S10, Supporting Information) that could be ascribed to  $^3\text{3-NA}$ . The absorbance of  $^3\text{3-NA}$  was barely affected by the presence of increasing amounts of pyrene, which is consistent with the low-contribution of singlet–singlet energy transfer from  $^1\text{Py}$  to 3-NA. Neither did the  $^3\text{3-NA}$  lifetime

change in the presence of pyrene, which shows the non-occurrence of triplet–triplet energy from  $^3\text{3-NA}$  to pyrene.

In the case of 4-NA, the  $S_1 \rightarrow S_0$  process is highly forbidden compared with intersystem crossing to the triplet.<sup>[10]</sup> The intersystem crossing and internal conversion times and the  $S_1 \rightarrow T_1$  intersystem crossing efficiency values for 4-NA in dioxane have been estimated as  $\leq 0.8$ ,  $\leq 0.5$  and  $\geq 0.40$  ps, respectively.<sup>[28]</sup> As expected, we did not detect fluorescence of  $^1\text{4-NA}$  at room temperature, but we registered the  $^3\text{4-NA}$  absorption spectrum in dioxane. The lifetime of about 300 ns was similar to that reported in the literature.<sup>[28,29]</sup> However, we failed to monitor clearly the effect of pyrene on the  $^3\text{4-NA}$  formation or its lifetime, due to pyrene bleaching and fluorescence. Interestingly, the  $^3\text{Py}$  yield was barely affected by the presence of 4-NA and, although triplet–triplet energy from  $^3\text{4-NA}$  to pyrene could not be completely discarded, once again, our data pointed to an enhanced intersystem crossing to the  $^3\text{Py}$  via  $^1\text{Py}$ –4-NA exciplexes.

Finally, we detected neither  $^1\text{2-NA}$  fluorescence at room temperature nor the  $^3\text{2-NA}$  absorption spectrum. Once again, the  $^3\text{Py}$  absorbance was barely affected by the presence of 2-NA, and this suggests an important contribution of  $^1\text{Py}$ –2-NA exciplexes in the formation of  $^3\text{Py}$ .

### 3. Conclusions

The above-mentioned data demonstrate that the efficiency of NAs as quenchers of pyrene fluorescence in low-polar solvents, such as toluene and 1,4-dioxane, correlates better with the NA dipole moment, which decreases in the order: 2-M-4-NA > 4-NA  $\gg$  3-NA > 4-M-3-NA > 4-M-3,5-DNA > 2-NA,<sup>[9]</sup> or even their hyperpolarizability ( $\beta$ ), which decreases in the order: 4-NAs > 2-NA > 3-NA,<sup>[30]</sup> than with their redox potential, which decreases

in the order: 3-NA > 2-NA > 4-NA (see Table S1 of the Supporting Information).

These chromophores possess a strong  $\pi$ -electron delocalization and intramolecular charge transfer stimulated by the presence of electron-donor and electron-acceptor groups. This is particularly relevant for the 4-NAs, whose apparent static quenching of pyrene fluorescence is consistent with their close proximity to the fluorophore at the ground state. Our data shows that NAs establish strong interactions, not only with the pyrene singlet excited state, but some NAs can also establish interactions with the Py ground state.

## Acknowledgements

We thank MICINN (Project CTQ2011-27758 and RyC contract to R.E.G) and GVA (Project GVACOMP/2011/269, Santiago Grisolia grant to C.E.A.) for their support.

**Keywords:** absorption · fluorescence spectroscopy · nitroanilines · pyrene · quenching

- [1] A. Airinei, R. I. Tigoianu, E. Rusu, D. O. Dorohoi, *Digest J. Nanomaterials and Biostructures* **2011**, *6*, 1265.
- [2] H. Li, Y. Li, *Nanoscale* **2009**, *1*, 128.
- [3] G. Xiang, C. Tong, H. Lin, *J. Fluoresc.* **2007**, *17*, 512.
- [4] G. R. Seely, *J. Phys. Chem.* **1969**, *73*, 125.
- [5] D. Patra, A. K. Mishra, *Sens. Actuators B* **2001**, *80*, 278.
- [6] H. M. Huang, K. M. Wang, S. S. Huang, L. J. Zhou, D. Li, *Anal. Chim. Acta* **2003**, *481*, 109.
- [7] M. O. Iwunze, M. Lambert, E. F. Silversmith, *Monatsh. Chem.* **1997**, *128*, 585.
- [8] V. K. Turchaninov, A. I. Vokin, T. N. Aksamentova, I. G. Krivoruchka, A. M. Shulunova, L. V. Andriyankova, *Russ. J. Gen. Chem.* **2003**, *73*, 743.
- [9] Y. Xiu-Fen, X. He-Ming, J. Xue-Hai, G. Xue-Dong, *Chin. J. Chem.* **2005**, *23*, 947.
- [10] O. S. Khalil, S. P. McGlynn, *J. Lumin.* **1975**, *11*, 185.
- [11] A. Jbarah, R. Holze, *J. Solid State Electrochem.* **2006**, *10*, 360.
- [12] C. Bohne, E. B. Abuin, J. C. Scaiano, *J. Am. Chem. Soc.* **1990**, *112*, 4226.
- [13] S. L. Murov, I. Carmichael, G. L. Hug, *Handbook of Photochemistry*, Second ed., New York, **1993**.
- [14] K. Kalyanasundaram, J. K. Thomas, *J. Am. Chem. Soc.* **1977**, *99*, 2039.
- [15] P. Deo, N. Deo, P. Somasundaran, S. Jockusch, N. J. Turro, *J. Phys. Chem. B* **2005**, *109*, 20714.
- [16] B. Schazmann, N. Alhashimy, D. Diamond, *J. Am. Chem. Soc.* **2006**, *128*, 8607.
- [17] S. H. Lee, S. H. Kim, S. K. Kim, J. H. Jung, J. S. Kim, *J. Org. Chem.* **2005**, *70*, 9288.
- [18] K.-S. Focsaneanu, J. C. Scaiano, *Photochem. Photobiol. Sci.* **2005**, *4*, 817.
- [19] M. S. Meaney, V. L. McGuffin, *Anal. Chim. Acta* **2008**, *610*, 57.
- [20] W. Chen, N. B. Zuckerman, J. P. Konopelski, S. Chen, *Anal. Chem.* **2010**, *82*, 461.
- [21] J. H. Lee, E. R. Carraway, M. A. Schlautman, S. Yim, B. E. Herbert, *J. Photochem. Photobiol. A* **2004**, *167*, 141.
- [22] S. Abraham, R. G. Weiss, *Photochem. Photobiol. Sci.* **2012**, DOI: 10.1039/c1pp05312d.
- [23] G. Pistolis, A. Malliaris, *Langmuir* **2002**, *18*, 246.
- [24] M. C. Cuquerella, S. E. Amrani, M. A. Miranda, J. Pérez-Prieto, *J. Org. Chem.* **2009**, *74*, 3232.
- [25] A. Goyal, M. Singh, *Ind. J. Chem.* **2007**, *46A*, 60.
- [26] O. S. Khalil, C. J. Seliskar, S. P. McGlynn, *J. Chem. Phys.* **1973**, *58*, 1607.
- [27] B. K. M. Szostak, G. Wojcik, J. Lipinski, *J. Chem. Soc. Faraday Trans.* **1998**, *94*, 3241.
- [28] C. L. Thomsen, J. Thøgersen, S. R. Keiding, *J. Phys. Chem. A* **1998**, *102*, 1062.
- [29] W. Schuddeboom, J. M. Warman, H. A. M. Biemans, E. W. Meijer, *The Journal of Physical Chemistry* **1996**, *100*, 12369.
- [30] W. Nie, *Adv. Mater.* **1993**, *5*, 520.

Received: August 6, 2012

Revised: September 24, 2012

Published online on October 22, 2012